Supporting Information for "Disruption and re-accretion of mid-sized moons during an outer Solar System Late Heavy Bombardment"

N. Movshovitz,[1] F. Nimmo,[1] D. G. Korycansky,[1] E. Asphaug,[2] and J. M. Owen[3]

Appendix A: Gravity-regime impact simula -tions with SPHERAL

SPHERAL++ is a Lagrangian, ASPH based hydrocode coupled with an oct-tree gravitational code. The Adaptive SPH algorithm, originally developed for cosmological applications, is described in [*Owen et al.*, 1998; *Owen*, 2010].

For the gravity-regime collisions of interest in this work, we made some modifications to the original, cosmological code. These include:

1. Addition of an equation-of-state for ice and rock. We implemented the Tillotson EOS [*Tillotson*, 1962; *Melosh*, 1989]. For water ice and for basalt we use the parameters suggested by *Benz and Asphaug* [1999, their Table II]. Because the Tillotson EOS is fully analytical, it is very computationally efficient and easy to implement. It may not be as complete or as accurate as the latest tabulated equations-of-state [*Senft and Stewart*, 2008], however, given the mixed composition of our targets (they are surely neither pure ice not pure rock) and the fact that we are interested in an order-of-magnitude question only, we chose expediency over thermodynamical accuracy.

2. A gravity time step based on local accelerations instead of local densities. During and immediately following impact, the time steps in a simulation are limited by a sound speed criterion. In later stages, it is the gravity time scale that controls the time stepping. For large scale structures, some fraction of

$$t_{\rm grav} = (G\rho)^{-1/2}, \tag{A1}$$

where G is the gravitational constant and ρ is an average density, can be used. But when the structure contains high- and low-density regions, as in the case of a large sheet of ejected material, this criterion is not useful. We look instead at the local accelerations of each SPH node, and a time step that is some fraction of

$$t_{\rm acc} = \sqrt{L/a_{\rm max}}, \tag{A2}$$

where L is a length scale of the system and $a_{\rm max}$ is the maximum instantaneous acceleration of any SPH node.

3. Initial condition generators for a target in hydrostatic equilibrium. The targets we are interested in here are in the 200-2000 km range. In the upper end of this size range, giving a target an initial constant density at the start of the simulation will result in local velocities that are due to the target collapsing or expanding under its own weight, and having nothing to do with the impact. To resolve this, it is important to start the target as close to hydrostatic equilibrium as possible. In our case, because the targets are only slightly compressed at equilibrium, we can use the first-order approximation:

$$p(r) = \frac{2\pi}{3} G\rho^2 (a^2 - r^2), \tag{A3}$$

where p is the pressure at radial distance r from the center, ρ is the average density, and a is the satellite's radius. This pressure profile can then be inverted (numerically) using the chosen equation-of-state to yield a density profile that can be used for initial SPH node placement.

When setting initial positions of SPH nodes, it is also important to keep a constant distance between neighboring nodes. We have experimented with several methods of node placement, including (a) on a rectangular grid, (b) on spherical shells, (c) randomized placement with uniform spatial probability, and (d) an Hexagonal Close Packing arrangement. The Hexagonal Close Packing arrangement, trimmed to a spherical shape by removing nodes outside a given radius, seems to work best. It guarantees equal distance between all 12 immediate neighbors of a node, and avoids the artificial singularities that result from a rectangular grid, especially if impactor is slightly translated or rotated with respect to the target. We have not noticed any artificial behavior that can be attributed to the geometry.

Our targets consist of 160,000 nodes (60 nodes across) and the number of nodes in the impactors is chosen to match the mass-per-node with the target as closely as possible. This results in $\sim$2000 nodes in a 250 km impactor. We simulate head-on collisions, so the impactor is set right next to the target with their centers almost aligned. (We set the impactor a few degrees above the target to break the artificial lattice symmetry.)

We run a collision to a few gravity times post-impact and then look for the largest remaining gravitationally bound mass. To do this, we first move to a reference frame moving with the SPH particle of lowest potential energy. This particle represents the bottom of the potential well and is usually in the center of the original target material. The mass of particles with negative total energy in this reference frame is added up. This method may over- or underestimate the bound mass in certain situations, but it generally gives accurate results in our scenario.

In SPHERAL the smoothing length h for each node is advanced based on measuring distortions in the local particle spacing via moments of the point distribution [*Owen*, 2010] and is not guaranteed contain a fixed number of neighbors. We thus need to limit the maximum smoothing length $h_{\rm max}$ to avoid a situation where escaping nodes expand their smoothing length to encompass the entire simulated space. Typically, $h_{\rm max}$ is a few times the initial separation between nodes. For consistency, we then need to set a lower bound on node density:

$$\rho_{\rm min} = m_{\rm node}/h_{\rm max}^3. \tag{A4}$$

[1]Department of Earth and Planetary Sciences, University of California Santa Cruz, Santa Cruz, CA 95064, USA.

[2]School of Earth and Space Exploration, Arizona State University, Tempe, AZ 85287, USA.

[3]Lawrence Livermore National Laboratory, Livermore, CA 94550, USA.

0094-8276/15/$5.00

Of the two standard ways to calculate density in SPH simulations, we usually employ the method of integrating the continuity equation.

Appendix B: Comparison of disruption scaling laws

The scaling of Q_D^* used for most of this work is a velocity-independent function of target size only, derived by fitting a power law to the combined results of SPH simulations from this work and those of *Benz and Asphaug* [1999] (see the Method section in the main text and Appendix A for detail). In contrast, *Leinhardt and Stewart* [2012, hereafter LS12] derive a more complete scaling law that makes Q_D^* an increasing function of impact velocity. This scaling law implies that using a value of Q_D^* for a given target size from SPH simulations at a given velocity to predict the outcome of higher velocity impacts might overestimate the disruption.

To test this possibility we ran our baseline Monte-Carlo simulation using the LS12 disruption scaling. The procedure to determine the total mass remaining post-collision, M_{lr} is as follows.

Given the target mass and radius, R and M, the impactor mass and radius, r and m, the impact velocity v and the impact angle θ, we first calculate m' the mass in the volume of impactor intercepting the target:

$$l = (R + r)(1 - \sin\theta), \tag{B1}$$

$$\alpha = \begin{cases} \frac{3rl^2 - l^3}{4r^3}, & l < 2r, \\ 1, & \text{otherwise}, \end{cases} \tag{B2}$$

$$m' = \alpha m. \tag{B3}$$

Next we compare the impact velocity with $v'_{\rm esc}$ defined by

$$v'_{\rm esc} = \sqrt{2G(M + m')/(R + r)}. \tag{B4}$$

If $v < v'_{\rm esc}$ the result is perfect merging and $M_{lr} = M + m$. Next we calculate:

$$\rho_1 = 1000 \text{ kg/m}^3, \tag{B5}$$

$$R_{c1} = \Big(\frac{3(M + m)}{4\pi\rho_1}\Big)^{1/3}, \tag{B6}$$

$$Q^*_{RD,\gamma=1} = c^* \frac{4\pi}{5} \rho_1 G R_{c1}^2, \tag{B7}$$

where $c^* = 1.9$ and G is the gravitational constant. We also need the reduced mass μ and reduced interacting mass μ':

$$\mu = \frac{Mm}{M + m}, \tag{B8}$$

$$\mu' = \frac{Mm'}{M + m'}. \tag{B9}$$

The disruption critical energy for head-on impacts is

$$Q^*_{RD} = Q^*_{RD,\gamma=1} \Big(\frac{1}{4}\frac{(\gamma + 1)^2}{\gamma}\Big)^{\frac{2}{3\bar{\mu}} - 1}, \tag{B10}$$

with $\bar{\mu} = 0.35$, and the modified value for an oblique impact is

$$Q^{*\prime}_{RD} = Q^*_{RD} \Big(\frac{\mu}{\mu'}\Big)^{2 - \frac{3}{2}\bar{\mu}}. \tag{B11}$$

With the disruption criterion we can calculate the impact velocity at the onset of erosion:

$$Q_e = 2Q^{*\prime}_{RD}(1 - M/(M + m)), \tag{B12}$$

$$V_e = \sqrt{2Q_e(M + m)/\mu}. \tag{B13}$$

If the collision is *grazing* (defined by $\sin\theta > (R/(R + r))$) and $v < v_e$ then the predicted result is a hit-and-run collision and $M_{lr} \approx M$. Otherwise, we compare the impact velocity with the critical velocity for *super-catastrophic* collisions, defined by $M_{lr} = 0.1M$:

$$Q_{sc} = 2Q^{*\prime}_{RD}(1 - 0.1M/(M + m)), \tag{B14}$$

$$V_{sc} = \sqrt{2Q_{sc}(M + m)/\mu}. \tag{B15}$$

If $v > v_{sc}$ then we use the power law

$$M_{lr} = (M + m)\frac{0.1}{1.8^\eta}\Big(\frac{Q_R}{Q^{*\prime}_{RD}}\Big)^\eta, \tag{B16}$$

where $\eta = -1.5$ and $Q_R = \mu v^2/(2(M + m))$. Otherwise the collision is in the disruption regime and the linear relationship

$$M_{lr} = (M + m)\Big(1 - \frac{1}{2}\frac{Q_R}{Q^{*\prime}_{RD}}\Big) \tag{B17}$$

holds.

Figure S1 shows the fraction of Monte-Carlo runs that included at least one collision with energy greater than one, two, or three times Q_D^*. Comparing with figure 2 in the main text, we see that, as expected, using the velocity-dependent Q_D^* scaling of LS12 results in less severe destruction. We get many fewer catastrophic collisions for each target. However, the probability of getting at lease *one* catastrophic disruption remains high. Our conclusions about the implications of the LHB for the mid-sized moons therefore hold, regardless of the scaling law used.

It is worth noting that while the LS12 velocity-dependent formalism is much more complete than our simple power law scaling (eq. 2 in the main text), it is not necessarily more accurate when extrapolated to larger targets. Indeed, the LS12 scaling law does a poor job matching our own SPH simulations. For example, LS12 predicts that a 200 km radius projectile hitting a 1000 km radius target head-on would have to impact at about 40 km/s for a catastrophic disruption, while our simulations show the same level of destruction at only 13 km/s. So while we have no choice but to extrapolate to higher velocities, by using our modification to the *Benz and Asphaug* [1999] scaling we do not need to extrapolate to the target size.

Appendix C: The impactor size distribution

A normalized power law distribution is completely defined by its power index, α. A segmented power law is completely defined by several indices α_i and the corresponding break points r_i. Here we detail the complete procedure for obtaining the size and mass distributions of cometary impactors in the outer Solar System, including the drawing of a pseudo-random sample in computer code.

C1. The Iapetus Scaled Distribution

Based on crater counts on Iapetus, *Charnoz et al.* [2009] recommend the following differential distribution for the population of heliocentric comets presumably responsible, which they call the Iapetus Scaled Distribution (hereafter ISD):

$$\begin{cases} \frac{dN}{dr} & \propto r^{-2.5}, \quad 0 < r < r_1 = 7.5, \\ \frac{dN}{dr} & \propto r^{-3.5}, \quad r_1 < r < r_2 = 100, \\ \frac{dN}{dr} & \propto r^{-4.5}, \quad r_2 < r. \end{cases} \tag{C1}$$

In the above equation r is the comet's radius in kilometers, and $N(r)$ is the cumulative fraction of comets with radius greater than r.

Equation (C1) is not enough to uniquely define the distribution. We need to make one more assumption, which is that $N(r)$ is a power law too. (Alternatively, we can assume that the differential distribution is continuous, or that the proportionality in eq. (C1) is the same for all branches.) In general, for each branch in eq. (C1), $N(r)$ can be of the form

$$N(r) = c_i r^{-\alpha_i} + b_i,$$

with c_i and b_i undetermined constants. Continuity and normalization will provide some constraints, but not enough to completely fix N unless we require that N be a power law, i.e. that $b_i = 0$. With this choice we get

$$N(r) = \begin{cases} c_1 r^{-1.5}, & 0 < r < r_1, \\ c_2 r^{-2.5}, & r_1 < r < r_2, \\ c_3 r^{-3.5}, & r_2 < r, \end{cases} \tag{C2}$$

and continuity at the break points requires that $c_3 = r_2 c_2 = r_2 r_1 c_1$.

We have a problem with the limit $N(r \to 0) = \infty$. This power law cannot extend to arbitrarily small comets. To normalize the distribution we must choose a minimum comet size, $r_{\min}$, below which $N(r < r_{\min}) = 1$. We need to be careful with this choice, because setting $r_{\min}$ too small will fill up our population (and computer memory) with tiny comets, while choosing a too large $r_{\min}$ means our population will be missing some mass. We will return to this question later, when looking at the mass distribution. For now we keep $r_{\min}$ unspecified.

Knowing that $N(0 < r < r_{\min}) = 1$, and that $N(r)$ must be continuous at $r_{\min}$, we can finally write the complete normalized distribution:

$$N(r) = \begin{cases} 1, & r < r_{\min}, \\ r_{\min}^{1.5} r^{-1.5}, & r_{\min} < r < r_1, \\ r_1\, r_{\min}^{1.5} r^{-2.5}, & r_1 < r < r_2, \\ r_1 r_2\, r_{\min}^{1.5} r^{-3.5}, & r_2 < r. \end{cases} \tag{C3}$$

C2. The mass distribution

To find the normalized differential mass distribution we need to use the *unnormalized* size distribution first:

$$\tilde{N}_c(r) = N_{\rm tot} N_c(r), \tag{C4}$$

where $N_{\rm tot}$ is the total number of comets. We also use $N_c = 1 - N$ to make the integration cleaner. The parameter $N_{\rm tot}$ is usually unknown. Luckily, we will see that the product $N_{\rm tot} r_{\min}^{1.5}$ can be simply related to the total mass in the distribution, $M_{\rm tot}$, in the limit $r_{\min} \to 0$.

The mass $d\tilde{M}_c$ in comets with radii between r and $r + dr$ is

$$d\tilde{M}_c = \rho \frac{4\pi}{3} r^3 d\tilde{N}_c(r) = \rho \frac{4\pi}{3} N_{\rm tot} r^3 dN_c(r), \tag{C5}$$

where ρ is a comets' bulk density in kilograms per cubic kilometer. The normalized differential mass is

$$dM_c = \frac{d\tilde{M}_c}{M_{\rm tot}} = \rho \frac{4\pi}{3} \frac{N_{\rm tot}}{M_{\rm tot}} r^3 dN_c(r). \tag{C6}$$

Integrating, we find

$$M_c(R < r) = \int_0^r \frac{dM_c(r')}{dr'}\, dr' =$$

$$\rho \frac{4\pi}{3} \frac{N_{\rm tot} r_{\min}^{1.5}}{M_{\rm tot}} \begin{cases} 0, \\ r^{1.5} - r_{\min}^{1.5}, \\ r_1^{1.5} - r_{\min}^{1.5} + 5 r_1 r^{0.5} - 5 r_1^{1.5}, \\ r_1^{1.5} - r_{\min}^{1.5} + 5 r_1 r_2^{0.5} - 5 r_1^{1.5} - 7 r_1 r_2 r^{-0.5} + 7 r_1 r_2^{0.5}, \end{cases}$$

Now we can use the normalization requirement $M(\infty) = 1$ to eliminate $N_{\rm tot} r_{\min}^{1.5}$. If we denote

$$\eta^{-1} = -4 r_1^{1.5} + 12 r_1 r_2^{0.5} - r_{\min}^{1.5}, \tag{C8}$$

we can write the complete normalized mass distribution:

$$M_c(r) = \eta \begin{cases} 0, & r < r_{\min}, \\ r^{1.5} - r_{\min}^{1.5}, & r_{\min} < r < r_1, \\ -4 r_1^{1.5} - r_{\min}^{1.5} + 5 r_1 r^{0.5}, & r_1 < r < r_2, \\ -4 r_1^{1.5} - r_{\min}^{1.5} + \\ \quad + 12 r_1 r_2^{0.5} - 7 r_1 r_2 r^{-0.5}, & r_2 < r \end{cases} \tag{C9}$$

(remembering that r is measured in km), and the unnormalized distribution in terms of $M_{\rm tot}$:

$$\tilde{M}_c = M_{\rm tot} M_c.$$

For the ISD $\eta^{-1} \approx 818 - r_{\min}^{1.5}$.

Now we can finally take the limit $r_{\min} \to 0$. We couldn't do this before, because we know that, for a given total mass, as $r_{\min}$ goes to zero $N_{\rm tot}$ increases without limit. But now we know that $N_{\rm tot} r_{\min}^{1.5}$ does have a limit:

$$\lim_{r_{\min} \to 0} \rho \frac{4\pi}{3} \frac{N_{\rm tot} r_{\min}^{1.5}}{M_{\rm tot}} = 12 r_1 r_2^{0.5} - 4 r_1^{1.5},$$

or about 0.0012 for the ISD.

We were able to normalize the mass distribution without any reference to $r_{\min}$. We can see that in the ISD only about 0.1% of the mass is found in comets smaller than 1 km, and only about 3% of the mass is found in comets smaller than 10 km. This gives us some confidence in choosing a reasonably large $r_{\min}$ when working with the number distribution in practice.

C3. Generating a pseudo-random ISD sample

Consider the cumulative distribution function (CDF):

$$F(r) = 1 - N(r) = \begin{cases} 0, & r < r_{\min}, \\ 1 - r_{\min}^{1.5} r^{-1.5}, & r_{\min} < r < r_1, \\ 1 - r_1\, r_{\min}^{1.5} r^{-2.5}, & r_1 < r < r_2, \\ 1 - r_1 r_2\, r_{\min}^{1.5} r^{-3.5}, & r_2 < r. \end{cases} \tag{C10}$$

If X is a random variable with a uniform distribution on $[0, 1]$ then

$$R = F^{-1}(X) \tag{C11}$$

is a random variable with the CDF $F(r)$. To see this is true, evaluate the probability $P(R < r)$:

$$P(R < r) = P\big(F^{-1}(X) < F^{-1}(x)\big) = P(X < x) = x = F(r), \tag{C12}$$

where the last couple of steps are valid because F is monotonic and X is uniform. Thus, to draw a random radius, in kilometers, from the ISD, we can draw a uniform random x from $[0, 1]$ with a pseudo-random number generator and then compute

$$r = \begin{cases} r_{\min}, & x = 0, \\ \left(\frac{(1-x)}{r_{\min}^{1.5}}\right)^{-1/1.5}, & 0 < x < 1 - r_{\min}^{1.5} r_1^{-1.5}, \\ \left(\frac{(1-x)}{r_1 r_{\min}^{1.5}}\right)^{-1/2.5}, & 1 - r_{\min}^{1.5} r_1^{-1.5} < x < 1 - r_1 r_{\min}^{1.5} r_2^{-2}, \\ \left(\frac{(1-x)}{r_1 r_2 r_{\min}^{1.5}}\right)^{-1/3.5}, & 1 - r_1 r_{\min}^{1.5} r_2^{-2.5} < x. \end{cases} \quad \text{(C13)}$$

Figure S2 shows an empirical CDF of a pseudo-random sample of 10^7 radii drawn using this method. Compare with figure. (2) of *Charnoz et al.* [2009].

References

Benz, W., and E. Asphaug (1999), Catastrophic disruptions revisited, *Icarus*, *142*, 5–20.

Charnoz, S., A. Morbidelli, L. Dones, and J. Salmon (2009), Did Saturn's rings form during the Late Heavy Bombardment?, *Icarus*, *199*(2), 413–428, doi:10.1016/j.icarus.2008.10.019.

Leinhardt, Z. M., and S. T. Stewart (2012), Collisions Between Gravity-Dominated Bodies. I. Outcome Regimes and Scaling Laws, *Astrophys. J.*, *745*(1), 79, doi:10.1088/0004-637X/745/1/79.

Melosh, H. (1989), *Impact cratering: a geologic process*, 245 pp., Oxford University Press.

Owen, J. (2010), ASPH modeling of Material Damage and Failure, in *5th Int. SPHERIC SPH Work.*, pp. 297–304, Manchester, United Kingdom.

Owen, J., J. Villumsen, P. Shapiro, and H. Martel (1998), Adaptive smoothed particle hydrodynamics : Methodology. II., *Astrophys. J. Suppl. Ser.*, *116*, 155–209.

Senft, L. E., and S. T. Stewart (2008), Impact crater formation in icy layered terrains on Mars, *Meteorit. Planet. Sci.*, *43*(12), 1993–2013, doi:10.1111/j.1945-5100.2008.tb00657.x.

Tillotson, J. (1962), Metallic equations of state for hypervelocity impact, *Tech. rep.*, General Dynamics General Atomics Div, San Diego CA.

Corresponding author: N. Movshovitz, Department of Earth and Planetary Sciences, University of California Santa Cruz, Santa Cruz, CA 95064, USA. (nmovshov@ucsc.edu)

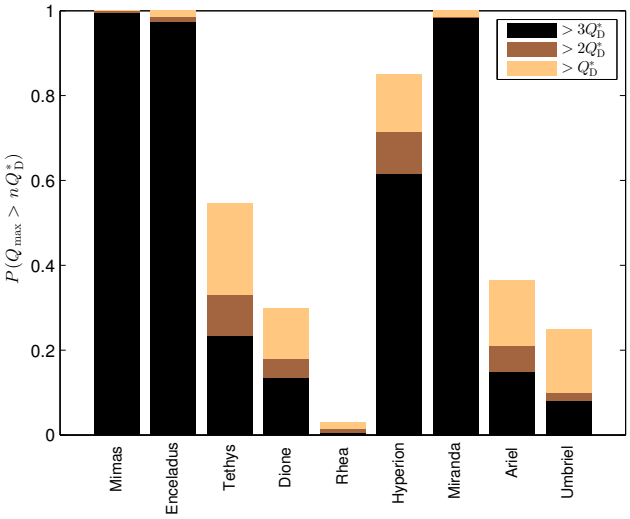

Figure S1. Fraction P of Monte-Carlo runs that included at least one impact with effective specific energy greater than one, two, or three times the catastrophic disruption threshold $Q_{RD}^{*\prime}$, eq. (B11). Compare with figure 2 in the main text.

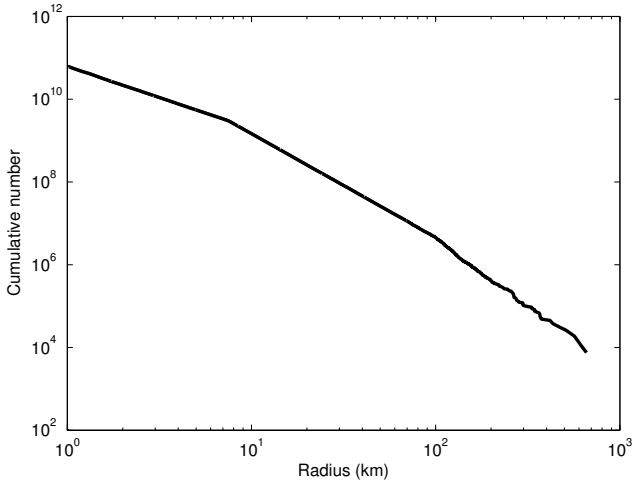

Figure S2. Cumulative number of comets with radii greater than a given value, summed from a pseudo-random sample of the distribution (C10) with $r_{\min} = 1$ and scaled to give 800 Pluto-or-larger ($r > 1100$ km) sized bodies.